2021 10th International IEEE/EMBS Conference on Neural Engineering (NER)
Virtual Conference, May 4-6, 2021

A segmented forearm model of hand pronation-supination approximates joint moments for real time applications*

Matthew G. Yough, Russell L. Hardesty, Sergiy Yakovenko, and Valeriya Gritsenko

Abstract— **Musculoskeletal modeling is a new computational tool to reverse engineer human control systems, which require efficient algorithms running in real-time. Human hand pronation-supination movement is accomplished by movement of the radius and ulna bones relative to each other via the complex proximal and distal radioulnar joints, each with multiple degrees of freedom (DOFs). Here, we report two simplified models of this complex kinematic transformation implemented as a part of a 20 DOF model of the hand and forearm. The pronation/supination DOF was implemented as a single rotation joint either within the forearm segment or separating proximal and distal parts of the forearm segment. Torques produced by the inverse dynamic simulations with anatomical architecture of the forearm (OpenSim model) were used as the "gold standard" in the comparison of two simple models. Joint placement was iteratively optimized to achieve the closest representation of torques during realistic hand movements. The model with a split forearm segment performed better than the model with a solid forearm segment in simulating pronation/supination torques. We conclude that simplifying pronation/supination DOF as a single-axis rotation between arm segments is a viable strategy to reduce the complexity of multi-DOF dynamic simulations.**

I. Introduction

Musculoskeletal models are useful tools in bottom-up descriptions of body mechanics for theoretical and engineering applications. A detailed biomechanical dynamic model of the human upper extremity was developed in OpenSim by Saul et al. [1], [2]. This and similar arm models have been used in human-machine interfaces [3]–[6] and biomimetic control systems for prosthetics [7]–[9]. This promising application embeds musculoskeletal models in closed-loop control systems, which can be implemented in Matlab (MathWorks, Inc.) with OpenSim application programming interface. Such hybrid control systems have been successfully implemented using both forward and inverse dynamic simulations [10]. However, each additional mechanical degree of freedom (DOF) in these models requires additional differential equations for simulating segmental dynamics. Solving these equations in real-time for closed-loop control of complex human anatomy remains challenging [11], [12]. For example, the human hand and forearm are comprised of 17 complex joints with at least 30 DOFs. Therefore, reducing the number of simulated DOFs is a practical means to simplify the implementation of biomimetic algorithms in closed-loop control systems. For example, pronation/supination of the wrist results from the rotation of both the ulna and radius along their respective longitudinal axes (2 DOFs). However, the resulting motion of the hand can be described as a single DOF about the forearm. Thus, it is possible to simulate the pronation/supination of the hand as a single-DOF revolute joint, reducing the number of differential equations that must be solved in real-time. The questions addressed in this study are how to define this hand/forearm simplification relative to the underlying anatomy and whether to model the forearm as one segment, as implemented in [13], or as two segments. These simplifications, however, still need to reflect accurately the joint moments produced by muscles. Body anatomy is embedded in the neural control signals [14], [15] and any mismatch between the intended biological and simulated forces will degrade the performance of a biomimetic system. Moreover, inverse simulations aimed at estimating muscle activity patterns and neural control signals from joint moments would be similarly affected by inaccuracies caused by model simplifications. In this study, we quantified the errors in predicting joint moments with inverse simulations that are caused by the simplification of pronation/supination as a single-DOF joint and developed a solution which reduced these errors.

II. Methodology

A. OpenSim Model

We used a published model of an arm with 3 joints and 7 DOFs that was implemented in OpenSim 4.1[1], [2]. The pronation/supination DOF was defined as a rotation of the radius about the ulna and the joint torque was measured about an axis parallel to the ulna segment (Fig. 1). To represent the variability of hand forces during naturalistic human movements we extended the model to articulate the hand with 16 DOFs, bringing the total number of DOFs to 20 as reported in [16]. The kinematic chain of hand segments was organized

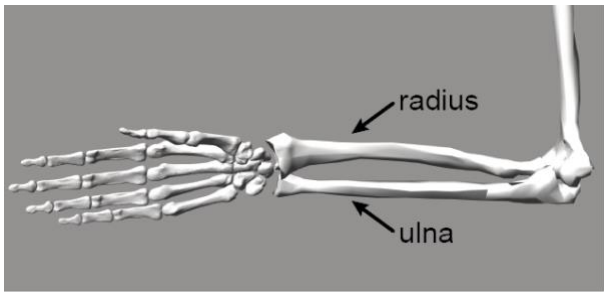

*Research supported by National Institute of General Medical Sciences and the National Institute of Child Health and Human Development.

M. G. Y. Author is with West Virginia University, Morgantown, WV 26506 USA (phone: 304-293-7976; fax: 304-293-7105; e-mail: mgy0003@mix.wvu.edu).

R. L. H. Author was with West Virginia University. He is now with the National Center for Adaptive Neurotechnologies, Stratton VA Medical Center, Albany, NY 12208 USA (e-mail: hardesty@neurotechcenter.org).

S. Y. Author is with West Virginia University, Morgantown, WV 26506 USA (e-mail: seyakovenko@mix.wvu.edu).

V. G. Author is with West Virginia University, Morgantown, WV 26506 USA (e-mail: vgritsenko@mix.wvu.edu).

2021 10th International IEEE/EMBS Conference on Neural Engineering (NER) | 978-1-7281-4337-8/21/$31.00 ©2021 IEEE | DOI: 10.1109/NER49283.2021.9441405

Authorized licensed use limited to: West Virginia University. Downloaded on July 21,2021 at 15:28:10 UTC from IEEE Xplore. Restrictions apply.

Figure 1. OpenSim model illustrating the anatomy of the forearm and hand segments. The pronation/supination is accomplished by radius rotating around the ulna.

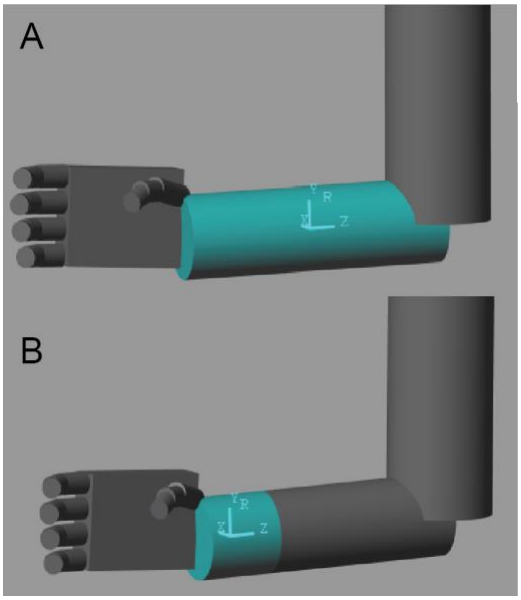

Figure 2. Two simplified models. A. Solid forearm Simulink model. Axes show a local coordinate system of the forearm segment. B. Segmented forearm Simulink model. Axes show a local coordinate system of the distal forearm segment.

from proximal segment (parent) to distal segment (child), i.e., from metacarpals, proximal phalanges, middle phalanges, and to distal phalanges. The segments of the hand that include carpal and metacarpal bones were modeled as a single rigid body with the inertia matrix of a rectangular prism (Fig. 2). The segments of digits were modeled as cylinders. The center of mass was placed in the center of each segment. The dimensions and inertial parameters of segments were based on published anthropometric data for humans of varied body sizes from 5% to 50% (average) to 95% of normal range [17], [18].

The joints were modeled as ideal joints with zero stiffness and viscosity. The carpometacarpal joint was modeled with two DOFs (thumb flexion/extension and abduction/adduction), and each of the rest of the 14 finger joints was modelled as hinge joints with one DOF (phalangeal flexion/extension). Local coordinate systems of bodies and joints were selected so that flexion was positive in all hand DOFs, and thumb abduction was positive.

B. Simulink Model

We developed two equivalent upper extremity models in Simulink (MathWorks, Inc). Both Simulink models matched the OpenSim model in all inertial and morphometric parameters with the exception of the forearm segment and pronation/supination joint. In the first Simulink model, referred to as solid forearm model, the forearm segment was a single cylinder with inertial parameters closely matched to the geometric sum of radius and ulna bodies of the OpenSim model (Fig. 2A). The center of mass was placed in the center of the forearm segment. The pronation/supination torque was measured between the humerus segment fixed in the world reference frame and the forearm segment about the Z axis in Fig. 2A. In the second Simulink model, referred to as segmented forearm model, the forearm segment from the first model was split into two cylinders (Fig. 2B). The pronation/supination torque was measured between the proximal and distal compartments of the forearm segment about the Z axis in Fig. 2B. The center of mass was placed in the center of each segment.

C. Inverse Dynamics

Movements of the hand were simulated to mimic characteristic point-to-point human movement with a bell-shaped velocity profile [19]. A total of 65 movements were simulated representing 13 hand movements each repeated at 0º, 45º, or 90º elbow flexion or with concurrent flexion or extension of elbow through 0º - 130º range. The simulated hand movements were as follows: 1) wrist pronation, 2) wrist supination, 3) wrist flexion and adduction, 4) wrist extension and abduction, 5) closing the hand, 6) opening the hand, 7) closing the hand and wrist pronation, 8) opening the hand and wrist pronation, 9) closing the hand and wrist supination, 10) opening the hand and wrist supination, 11) while in supination, closing the hand and flexing the wrist, 12) while in pronation, opening the hand and extending the wrist, and 13) hand opening while the thumb is flexing. The angular kinematics of each moving DOF for a given movement was approximated as a symmetrical sigmoidal trajectory in time lasting 0.5 seconds (Fig 3A). The trajectory was scaled in amplitude to the appropriate range for each movement. In most movements, the starting posture for all DOFs was a neutral, i.e., the half-way angle between the maximal and minimal range of the corresponding DOF. The stopping angle was at 45% of maximal or minimal range derived from published ergonomic data [18]. The polynomial coefficients of the scaled trajectory were then differentiated to calculate angular velocity and differentiated again to calculate angular acceleration. The angular position of the non-moving DOFs were set to the required posture (neutral posture, elbow at 0º, 45º, or 90º flexion angle, or full pronation or supination) with zero velocity and acceleration.

We computed applied joint torques for all models using inverse dynamics driven by angular kinematics of each of the 65 movements. Simulations with the OpenSim model were run using the inverse dynamics tool of OpenSim MATLAB API. The torques were low-pass filtered at 6 Hz. Simulations with the Simulink models were ran using 4th order Runge-Kutta solver with a fixed 1 ms timestep. Simulations with models of different body sizes were ran to test the generality of our conclusions for the analysis of kinematic data from individuals of different sizes. The OpenSim and Simulink joint torques were compared by calculating root-mean-squared-error (RMSE) for each DOF for all movements. The RMSE values were normalized to the torque range of the OpenSim model per DOF per movement.

III. RESULTS

Applied torques calculated with inverse dynamics were on similar scale across all models for all movements. The mean RMSEs were below 5% of peak-to-peak torque for most DOFs across all movements. This shows that the inverse dynamic calculations in OpenSim API and Simulink are similar despite any differences in their respective algorithms. The differences between models were, as expected, primarily in pronation-supination torques.

The applied torque about the pronation/supination DOF of the segmented model was the most similar to that produced by anatomical joints simulated in OpenSim (Fig. 3B). The

Authorized licensed use limited to: West Virginia University. Downloaded on July 21,2021 at 15:28:10 UTC from IEEE Xplore. Restrictions apply.

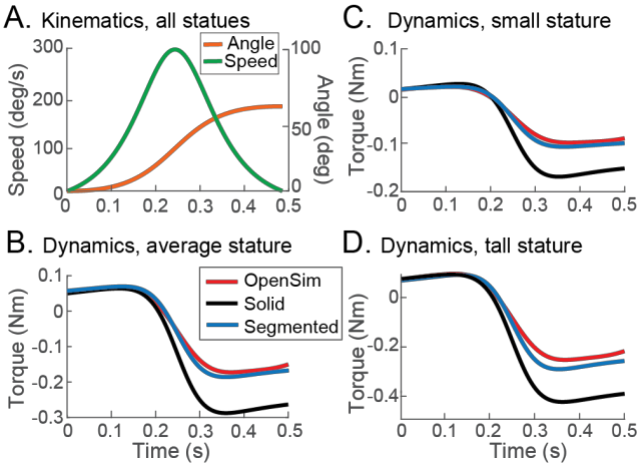

Figure 3. Trajectories for pronation/supination DOF from inverse dynamic simulation of a movement 1) as described in methods with elbow at 90°. A. Angular kinematics that served as input into the simulation (acceleration is not shown). B. Applied torque, the output of the simulations with the OpenSim and two Simulink models (solid and segmented) scaled to the average body size (50th percentile of normal range). C & D. Same as B for models scaled to the small and tall body size respectively (5 and 95th percentiles respectively).

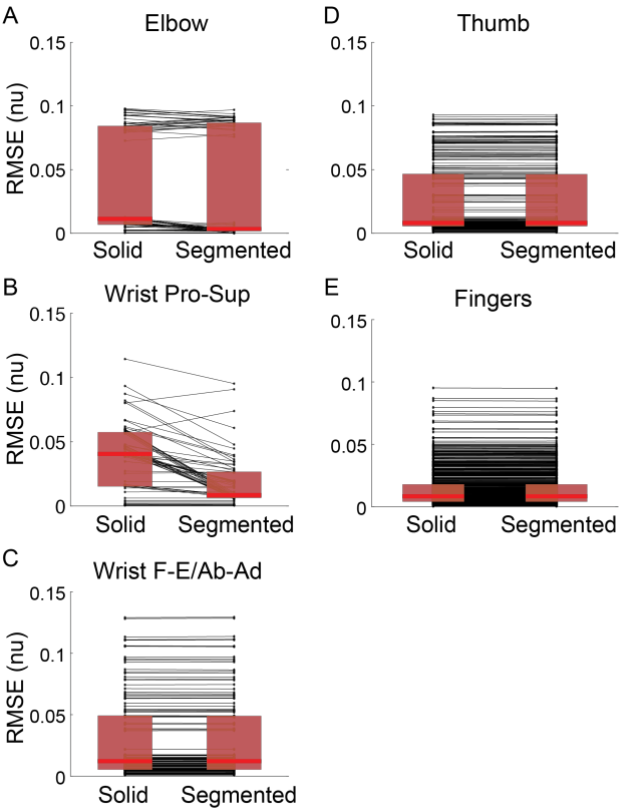

Figure 4. Torque errors between solid and segmented Simulink models and OpenSim model. A-E: Errors for torques about individual joints. Black lines connect RMSE values for corresponding movements, red lines are averages with shaded rectangles indicating interquartile range. Pro-Sup indicated pronation and supination; F-E indicated flexion and extension; Ab-Ad indicates abduction and adduction; nu indicated normalized units.

forearm architecture had a generally small effect on the torque accuracy across all movement and DOFs (Fig. 4). As expected, the largest effects of forearm architecture on torque accuracy across all movements was at pronation/supination and elbow DOFs (Fig. 4A & B). These errors were driven by the differences in offset, as illustrated in Fig. 3B, or in profiles that affected the peak values of applied torques and sometimes both. This shows that simulations with solid forearm models could be wrong by up to 15% in estimating the amplitude of postural and propulsion-related muscle forces.

Torque profiles obtained for the models of short and tall human body sizes varied in scale, but not profiles (Fig. 3C & D). The errors between the corresponding OpenSim and segmented models generally increased with body size but remained mostly below 15% of peak-to-peak torque (Fig. 5). The scaling of errors with body size was the most prominent in torques about the wrist and finger joints in movements with concurrent elbow motion. This is likely due to the cumulative effect of numerical errors that propagate from proximal to distal joints and have a larger effect on smaller distal torques.

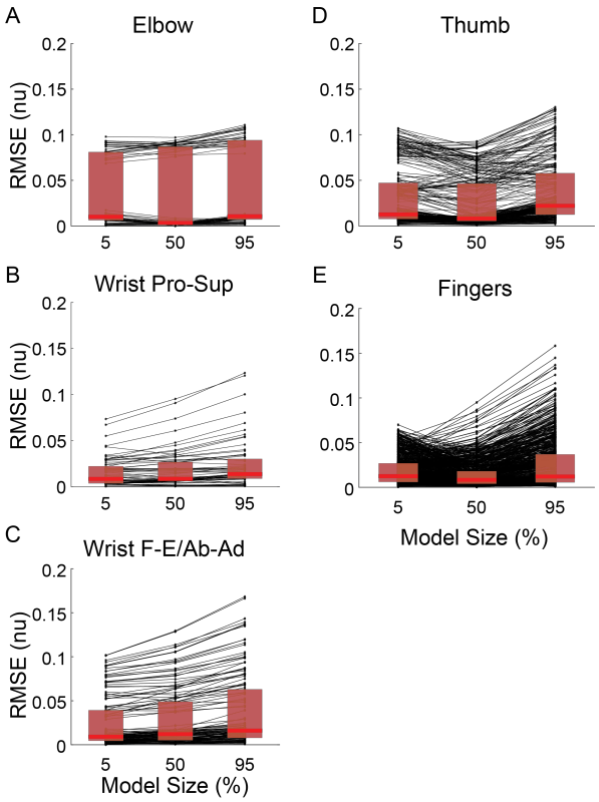

Figure 5. Torque errors between segmented Simulink model and the corresponding OpenSim model scaled to short (5%), average (50%), and tall (95%) body sizes. Formatting as in Figure 4.

IV. Discussion and Conclusion

Despite known difficulties in obtaining consistent solutions across platforms [20], we have achieved very close inverse simulation results between OpenSim and Simulink models. Even the model with extremely simplified pronation/supination joint placed in the cylindrical solid forearm segment produced joint torques that were closely matched to those of a model with separate ulna segment rotating about the radius segment through complex joints (Fig. 4). These errors were mostly below 10% of peak-to-peak torques across all simulated joints and movements, with

Authorized licensed use limited to: West Virginia University. Downloaded on July 21,2021 at 15:28:10 UTC from IEEE Xplore. Restrictions apply.

pronation/supination being the most adversely affected DOF. Our results have shown that when the accuracy of muscle moments about the wrist is not crucial, a simplified pronation/supination joint with a single DOF placed in the elbow can provide reasonable approximations for biomedical applications.

The segmented forearm model in Simulink performs with high precision across all tested movements. The errors were within the range of perceptual errors in joint position measured in psychometric human studies [21]. The uneven split into proximal and distal cylindrical segments closely matches the moments of inertia of the radius segment rotating about the ulna segment and results in the smallest errors between OpenSim and Simulink models (Fig. 4). This model still simulates pronation/supination as a single DOF about an axis parallel to both compartments of the forearm segment, providing the benefit of a simplified dynamic simulation. This result has direct implications for neuroprostheses. The myoelectric control of actuated hand prostheses in transradial amputees may be improved by embedding the segmented model into the decoding algorithm. Such a model could be more accurate in predicting the intended motion from contractions of residual muscles involved in pronation and supination, such as pronator teres, supinator, biceps, and extensor and flexor carpi radialis and ulnaris muscles.

The accuracy of simulations with movement of the elbow were sensitive to body size. In these movements, the errors scaled with model size by less than 1% on average, the worst single-movement simulation showing 15% errors about finger joints (Fig. 5E). This cannot be explained by the change in body inertia because RMSE values were normalized to the peak-to-peak torque, which scaled with body size. This normalization did not remove the trend, indicating that the errors in numerical methods for solving differential equations may be the culprit. Our results show that the cumulative effect of these numerical errors in simulations with movement of proximal joints is the largest at distal joints.

In conclusion, both the solid and segmented forearm models performed well in simulating applied joint torques during naturalistic human movements, below 5% errors on average. The segmented model is preferred for applications where accuracy in the muscle moments driving pronation or supination is important. This performance is good enough for dynamic real-time simulations, for example, in biomimetic controllers. Both types of models can be scaled for individual body size with minimal reduction in the accuracy of dynamic simulations.

REFERENCES

[1] K. R. Saul *et al.*, "Benchmarking of dynamic simulation predictions in two software platforms using an upper limb musculoskeletal model," *Comput. Methods Biomech. Biomed. Engin.*, vol. 18, no. 13, pp. 1445–1458, Oct. 2015, doi: 10.1080/10255842.2014.916698.

[2] K. R. S. Holzbaur, W. M. Murray, and S. L. Delp, "A Model of the Upper Extremity for Simulating Musculoskeletal Surgery and Analyzing Neuromuscular Control," *Ann. Biomed. Eng.*, vol. 33, no. 6, pp. 829–840, Jun. 2005, doi: 10.1007/s10439-005-3320-7.

[3] T. Kapelner, M. Sartori, F. Negro, and D. Farina, "Neuro-Musculoskeletal Mapping for Man-Machine Interfacing," *Sci. Rep.*, vol. 10, no. 1, p. 5834, Dec. 2020, doi: 10.1038/s41598-020-62773-7.

[4] A. J. Nelson, P. T. Hall, K. R. Saul, and D. L. Crouch, "Effect of Mechanically Passive, Wearable Shoulder Exoskeletons on Muscle Output During Dynamic Upper Extremity Movements: A Computational Simulation Study," *J. Appl. Biomech.*, vol. 36, no. 2, pp. 59–67, Apr. 2020, doi: 10.1123/jab.2018-0369.

[5] L. Peternel, C. Fang, N. Tsagarakis, and A. Ajoudani, "A selective muscle fatigue management approach to ergonomic human-robot co-manipulation," *Robot. Comput.-Integr. Manuf.*, vol. 58, pp. 69–79, Aug. 2019, doi: 10.1016/j.rcim.2019.01.013.

[6] R. J. Varghese, B. P. L. Lo, and G.-Z. Yang, "Design and Prototyping of a Bio-Inspired Kinematic Sensing Suit for the Shoulder Joint: Precursor to a Multi-DoF Shoulder Exosuit," *IEEE Robot. Autom. Lett.*, vol. 5, no. 2, pp. 540–547, Apr. 2020, doi: 10.1109/LRA.2019.2963636.

[7] D. Blana, J. G. Hincapie, E. K. Chadwick, and R. F. Kirsch, "A musculoskeletal model of the upper extremity for use in the development of neuroprosthetic systems," *J. Biomech.*, vol. 41, no. 8, pp. 1714–1721, 2008, doi: 10.1016/j.jbiomech.2008.03.001.

[8] E. K. Chadwick, D. Blana, A. J. van den Bogert, and R. F. Kirsch, "A Real-Time, 3-D Musculoskeletal Model for Dynamic Simulation of Arm Movements," *IEEE Trans. Biomed. Eng.*, vol. 56, no. 4, pp. 941–948, Apr. 2009, doi: 10.1109/TBME.2008.2005946.

[9] M. Fadzli, A. Hanafusa, Y. Kubota, and D. Nishimori, "Preliminary Study on Muscle Force Estimation using Musculoskeletal Model for Upper Limb Rehabilitation with Assistive Device for Home Setting," *J. Phys. Conf. Ser.*, vol. 1372, p. 012023, Nov. 2019, doi: 10.1088/1742-6596/1372/1/012023.

[10] M. Mansouri and J. A. Reinbolt, "A platform for dynamic simulation and control of movement based on OpenSim and MATLAB," *J. Biomech.*, vol. 45, no. 8, pp. 1517–1521, May 2012, doi: 10.1016/j.jbiomech.2012.03.016.

[11] D. Blana, E. K. Chadwick, A. J. van den Bogert, and W. M. Murray, "Real-time simulation of hand motion for prosthesis control," *Comput. Methods Biomech. Biomed. Engin.*, vol. 20, no. 5, pp. 540–549, Apr. 2017, doi: 10.1080/10255842.2016.1255943.

[12] A. J. van den Bogert, D. Blana, and D. Heinrich, "Implicit methods for efficient musculoskeletal simulation and optimal control," *Procedia IUTAM*, vol. 2, no. 2011, pp. 297–316, Jan. 2011, doi: 10.1016/j.piutam.2011.04.027.

[13] A. Biess, D. G. Liebermann, and T. Flash, "A Computational Model for Redundant Human Three-Dimensional Pointing Movements: Integration of Independent Spatial and Temporal Motor Plans Simplifies Movement Dynamics," *J. Neurosci.*, vol. 27, no. 48, pp. 13045–13064, Nov. 2007, doi: 10.1523/JNEUROSCI.4334-06.2007.

[14] K. Nishikawa *et al.*, "Neuromechanics: an integrative approach for understanding motor control," *Integr. Comp. Biol.*, vol. 47, no. 1, pp. 16–54, May 2007, doi: 10.1093/icb/icm024.

[15] R. M. Enoka, *Neuromechanics of human movement*, Fifth edition. Champaign, IL: Human Kinetics, 2015.

[16] V. Gritsenko, R. L. Hardesty, M. T. Boots, and S. Yakovenko, "Biomechanical Constraints Underlying Motor Primitives Derived from the Musculoskeletal Anatomy of the Human Arm," *PLOS ONE*, vol. 11, no. 10, p. e0164050, Oct. 2016, doi: 10.1371/journal.pone.0164050.

[17] D. A. Winter, *Biomechanics and Motor Control of Human Movement*, 4th ed. Wiley, 2009.

[18] Kodak, "Ergonomics Design Philosophy," in *Kodak's Ergonomic Design for People at Work*, John Wiley & Sons, Ltd, 2007, pp. 1–98.

[19] E. V. Olesh, B. S. Pollard, and V. Gritsenko, "Gravitational and Dynamic Components of Muscle Torque Underlie Tonic and Phasic Muscle Activity during Goal-Directed Reaching," *Front. Hum. Neurosci.*, vol. 11, p. 474, 2017, doi: 10.3389/fnhum.2017.00474.

[20] D. W. Wagner *et al.*, "Consistency Among Musculoskeletal Models: Caveat Utilitor," *Ann. Biomed. Eng.*, vol. 41, no. 8, pp. 1787–1799, Aug. 2013, doi: 10.1007/s10439-013-0843-1.

[21] V. Gritsenko, N. I. Krouchev, and J. F. Kalaska, "Afferent Input, Efference Copy, Signal Noise, and Biases in Perception of Joint Angle During Active Versus Passive Elbow Movements," *J. Neurophysiol.*, vol. 98, no. 3, pp. 1140–1154, Sep. 2007, doi: 10.1152/jn.00162.2007.

Authorized licensed use limited to: West Virginia University. Downloaded on July 21,2021 at 15:28:10 UTC from IEEE Xplore. Restrictions apply.